2024; Vol 13: Issue 8

Open Access

# Advanced Deep Neural Network Approaches for Classification and Denoising of Microscopic Malaria-Infected Cells in Thin Blood Smear Imaging

## Muhammad Shameem P1, Dr. Mathiarasi Balakrishnan2\*

<sup>1</sup>Research Scholar, Hindustan University, Department of CSE, Chennai, India. <sup>2\*</sup>Assistant Professor (Selection Grade), Hindustan University, Department of CSE, Chennai, India.

Cite this paper as: Muhammad Shameem P, Dr. Mathiarasi Balakrishnan (2024). Advanced Deep Neural Network Approaches for Classification and Denoising of Microscopic Malaria-Infected Cells in Thin Blood Smear Imaging. Frontiers in Health Informatics, 13 (8) 3095-3111

ABSTRACT: Image denoising poses a major challenge in the field of medical imaging, particularly when analyzing thin blood smear images to detect malaria-infected cells. Most traditional noise-freezing methods cannot accomplish image noise-freezing because the various noise types in medical images are too complex. This study presents a dedicated noise-freezing approach that leverages state-of-the-art deep neural network architectures to noise-freeze images of malaria-infected cells in thin blood smears. It uses a two-network method. The first network is designed to identify and classify some of the most prevalent noise types in the medical imaging field: speckle noise, salt and pepper noise, Poisson noise, and Gaussian noise. The first network helps to classify the noise, and based on the previous classification, the second network performs noise-freezing using the information from the first network to effectively remove the identified noise types. This customized method approach aims to provide a solution to these challenges while dealing with the specific noise types provided by images of malaria-infected cells. The results show that in addition to producing higher accuracy in classifying noise, the high quality of noise-free images has also improved significantly.

**Keywords:** Deep Convolutional Neural Networks (CNN), Quantitative Image Quality Metrics (PSNR, SSIM), Swish Activation Function, Sparsemax for Classification, Residual Learning for Image Denoising

#### 1. Introduction

Data acquisition errors cause loss of information and make it hard to characterize the tissue or other features of interest hence, extracting useful and interpretable information from noisy images still is and always remains an important problem of image analysis and has important implications for medical diagnosis. Image denoising: One of the important preliminary steps in image processing to removing noise artifacts and preserving the structure and texture of the actual information presented. This step is crucial for medical imaging since the quality and reliability of visual data directly affect the accuracy of diagnosis and the results of the decision-making process. (Muksimova et al., 2023). In thin blood smear images used for malaria diagnosis, noise hides important visual cues and disrupts the entire diagnosis process. Noise in medical images has different origins including limitations of imaging modalities, poor acquisition conditions, and noise from the environment in the process of capturing images. This can lead to a variety of noise types including speckle noise, salt-and-pepper noise, Poisson noise, and Gaussian noise, each one bringing its complications to the process of detection and removal. Common noise in ultrasound imaging is Speckle noise caused by constructive and destructive interference of coherent waves whereas salt-andpepper is usually based on defective transmission or due to hardware faults. For example, in the case of a thin blood smear where morphological characteristics of invading cells might be faint, these noise artifacts can occlude small features so critical for accurate testing and diagnosis of conditions such as malaria (Magsood et al., 2021; Poostchi et al., 2018). Traditional noise-removal techniques often rely on well-established hypotheses about the type of noise

2024; Vol 13: Issue 8 Open Access

and its statistical properties. These include linear or non-linear filtering, wavelet-based methods, and optimization methods. Although such methods can provide adequate results for certain noise types, their performance often deteriorates when it is subjected to the complex and varied characteristics of noise in particular medical images (Wachowiak et al., 2000). Moreover, these approaches have a limitation in that they have to compromise between noise reduction and non-edge smoothing since more smoothing will remove the important edges and less smoothing will keep the noise. This shortcoming of traditional methods points towards the requirement of sophisticated noise-removal techniques designed to address the complexities of medical imaging (Abuya et al., 2023).

This research introduces a new approach based on state-of-the-art deep neural networks to the problem of medical image noise stabilization, specifically applied to malaria-infected thin blood smear images. With deep learning, hierarchical representations can be learned directly from the data, and hence the model can adapt to different types of noise without requiring any fixed and hand-crafted assumptions. Unlike existing noise-stabilization methods, our dual-network framework benefits from the complementary nature of domain-specific knowledge and data-driven learning. The noise classification network in the framework is deepened to accurately classify noise types, and then a noise-specific noise-stabilization network is built to remove the classified noise while preserving essential image details. This modular, adaptive architecture can learn diverse noise patterns in malaria diagnosis data, preserving features essential for malaria diagnoses, such as cell morphology- and parasite structures. Through experiments, it shows that our method achieves excellent classification accuracy of noise compared with existing methods while generating visually pleasing noise-free images and outperforming other methods, thereby increasing the reliability and efficiency of malaria diagnosis.

## 2. Literature Review

Malaria, an infectious disease caused by parasites of the Plasmodium genus and sometimes fatal, has traditionally been diagnosed through microscopic blood smear examination a practice that dates back to the late 19th century. This approach was established in the early days of parasitology and has become indispensable for malaria parasites due to its unique ability to determine not only the absolute rather than the relative amount of presence but also species and stage specificity. The gold standard for malaria diagnosis is recognized primarily due to the high-resolution capability of microscopic examination which can demonstrate even the smallest features of parasite morphology. Being able to discern species differences and disease severity is particularly important with this capability (Sato, 2021).

Microscopy is still an indispensable component in the diagnosis of malaria, although more advanced diagnostics such as polymerase chain reaction (PCR) assays, rapid diagnostic tests (RDTs), and automated imaging systems have been developed. Availability in many markets, relatively low cost, and provision of detailed diagnostic information in real-time all increase the flexibility of biochemical markers. Abstract Microscopy is complementary to clinical and epidemiological diagnosis, allowing quantification of parasite levels in treatment assessment, and is a valuable tool for malaria control programmers. This is particularly relevant in resource-scarce contexts, where the cost, technical complexity, or infrastructure demands of diagnostic machinery may make advanced diagnostics impractical (Fitri et al., 2022). Furthermore, microscopy is not limited to malaria diagnosis as it is capable of simultaneously identifying various blood-related abnormalities and, therefore, may prove to be even more robust in diagnostic laboratories. Whether microscopy or other diagnostic methods are developed, these features follow the trends seen in diagnosis as tools in the war against malaria become more advanced (Plucinski et al., 2021).

Thin blood smears are made by spreading the blood sample from a patient in a monolayer on a microscope slide and staining it to visualize the Plasmodium parasites and is inimitable for the microscopic diagnosis of malaria. It appears to be pretty simple, but you have to go through a lot of technical accuracy and there is so much expertise involved if the work needs to be done accurately. Smear preparation is important as it affects the identification of systematic and intracellular details of the staining method (Shimizu et al., 2011). A good smear will show blood cells separately, i.e. one cell will appear above another. Variation in smear thickness varies the thickness of the blood, smears made with

improperly preserved blood viscosity may not stain uniformly and will hide the parasites or make them difficult to detect. Another important factor would be the quality of the blood sample, many factors such as hemolysis, clotting, or improper handling of blood can impair the quality of the sample and smear and subsequently affect the staining results.

Table 1: Types of noise in microscopic images, their characteristics, origins, and impact on malaria diagnosis.

SN	Type of Noise	Characteristics and Origins	Impact on Malaria Diagnosis
1	Speckle Noise	Granular interference appearing in imaging modalities like ultrasound and radar affects microscopic images due to irregularities in blood smears, such as inconsistencies in thickness or granularity.	Reduces image clarity, making it difficult to distinguish fine details of plasmodium parasites from the background, potentially leading to misdiagnosis.
2	Salt and Pepper Noise	Random occurrences of black and white pixels caused by digital sensor errors, debris, slide imperfections, or errors in image transmission/processing.	Mimics the appearance of parasites or obscures important features, complicating accurate identification of malaria-infected cells.
3	Poisson Noise	Also known as shot noise, inherent to the photon counting process, results from variations in illumination and detector sensitivity, leading to fluctuations in pixel intensities not reflecting true sample variation.	Causes loss of detail and contrast, especially in low signal regions, making it difficult to detect parasites, particularly those in early developmental stages.
4	Gaussian Noise	Resembles a random statistical distribution of pixel values, attributed to electronic circuit noise, sensor noise, and external environmental factors, which can also result from diffused light or fluctuations in imaging system performance.	Adds random variation to pixel values, reducing image sharpness and potentially masking subtle features necessary for accurate identification and classification of malaria parasites.

Microphotographic images contain a lot of noise caused by several sources, which can have serious consequences for the diagnosis of malaria. The types of noise are classified in Table 1 with important characteristics, possible sources, and clinical relevance. Detection of Plasmodium parasites from blood smears may not be accurate because of the presence of speckle noise, characterized by granular interference, which arises from the large field-of-view and high-contrast image characteristics of blood smears; salt-and-pepper noise, which is usually caused by sensor errors or defects on the slide and is randomly introduced into the image as black and white pixels that either mimic or hide features characteristic of the parasite (Singh & Shree, 2016; Toh & Isa, 2010). Originally inherited from photon-counting processes, this pixel-intensity variation causes Gaussian noise, typically introduced by electronic and environmental interference, which can randomly shift pixel values, degrading image sharpness and making important parasitic features indistinguishable (Boncelet, 2009; Le et al., 2007).

Noise reduction, which is essential in many applications such as medical imaging, has been performed for several

2024; Vol 13: Issue 8 Open Access

decades using traditional techniques. These processes use simple numerical and statistical methods to reduce unwanted background noise while trying to preserve important details of the image. Median filtering, median filtering, and Gaussian blurring are specific approaches, each of which provides different advantages for particular noise types (Cao & Liu, 2024; Shreyamsha Kumar, 2013). A good example of this is median filtering where a pixel value is replaced by the median of its neighboring values, it works well with salt-and-pepper noise. It effectively eliminates the sudden/random noise in the image, thus enhancing the output image. Similarly, median filtering uses pixel values in the neighborhood, and Gaussian blurring uses a weighted mean, giving more weight to neighbors. This is attractive, especially for resource-constrained application domains or real-time applications, because they are computationally efficient, easy to implement, and cheap. Although these classical techniques are very simple to use, this approach has some limitations when the noise is complex, for example, speckle noise or Gaussian noise that are commonly present in medical images. Unfortunately, their reliance on smoothing can also blur details of the smoothing process, thereby erasing the very features needed to accurately interpret images. While, for example, Gaussian blurring reduces noise by averaging pixel values, it also reduces small-scale information, such as the detailed morphology of cells or parasites in medical diagnosis. While median filtering is successful in removing random noise, it inadvertently blurs edges and important texture features in nature.

There have been sophisticated denoising algorithms such as wavelet transforms, adaptive filtering, supervised and unsupervised methods, simple convolution preprocessing, CNNs, and hybrid approaches. Wavelet transforms will help significantly to address image noise as they decompose an image into components in the frequency domain which enables noise reduction to be applied across scales (Shreyamsha Kumar, 2013). Wavelet transforms allow adaptive filtering by separating high-frequency components (associated with noise) from low-frequency components (associated with important image features). By this targeted approach, they improve their performance in reducing common noise types - Gaussian and speckle noise that commonly occur in medical images. Wavelet-based approaches strike an important balance between denoising and detrending, with a finiteness preservation aspect offering the promise of retaining fine details such as morphological features of cells or parasites.

An advanced solution in terms of noise reduction is adaptive filtering methods such as adaptive Wiener filtering. Such methods optimize their parameters according to the local mean and variance of the image. Adaptive filters differ from traditional filters with their fixed parameters because they optimize their actions for a specific part of the image, allowing for more targeted noise removal (Jin et al., n.d.). This gives good flexibility on images where the noise is not uniform - meaning that some areas may require stronger filtering than others. One of the main advantages of adaptive Wiener filtering is its ability to remove noise while maintaining edges and textures, which is important in medical images.

Machine-learning-based noise reduction has improved the arsenal of tools available to deal with complex noise signatures. These are supervised learning methods, such as support vector machines (SVMs), decision trees, and neural networks, where we need labeled datasets to train the model so that we can learn to discriminate between noise and signal (Rai et al., 2021). These approaches are particularly powerful in detecting and classifying different noise classes from microscopic images which helps in more adaptive and specific noise reduction. Supervised models learn from data with known noise behavior, allowing them to generalize their learning to previously unseen data, and they can be quite efficient when the noise behavior is consistent (Ilesanmi & Ilesanmi, 2021; Kaur et al., 2018).

When the datasets are unlabeled, it is also possible to reduce noise particles using some unsupervised learning methods, such as K-means clustering [17] and principal component analysis (PCA) [18]. They identify patterns and structures in unlabeled data, allowing noise to be removed from the raw data based on features alone. By transforming the data into a low-dimensional basis space, PCA retains the features of the data that are most important while filtering out other noisy features from the data. These methods are particularly effective in

2024; Vol 13: Issue 8 Open Access

exploratory scenarios in which noise properties are undefined (Ferzo & Abdulazeez, 2024; Linlin Xu et al., 2014). Deep learning approaches, especially convolutional neural networks (CNNs), have changed the way noise reduction is done by using their hierarchical structures to learn complex representations of data in images. CNNs are very powerful for multi-dimensional and complex data such as blood-related images that would be infected with malaria (Zhang et al., 2023). They can understand the spatial hierarchy and contextual relationships of image content and can thus separate noise from important features and provide high-quality noise-free images. These pose challenges especially in resource-constrained environments, as they have high computational requirements and require large and heterogeneous training datasets (P & Malarvel, 2024). Therefore, despite these limitations, CNNs remain attractive contenders for advanced noise-free applications.

Hybrid techniques have attracted attention because they have the potential to achieve a combination of the strengths of traditional and contemporary noise reduction strategies. A hybrid method can use classical filters such as median filtering to remove large noise, and then use machine learning models to further refine the results (Xu et al., 2020). The sequential nature of this process combines the efficiency and speed of classical methods with the accuracy and adaptability of modern algorithms. The hybrid approach is an effective way to minimize the disadvantages of individual techniques and is suitable for medical imaging, where local contrast must be preserved (P & Malarvel, 2023).

### Research Gap

Although deep neural networks have made great progress in medical imaging, classification and noise reduction of microscopic images of thin blood smears of malaria-infected blood cells is still a challenging task. Contemporary methods face challenges posed by factors such as very high variation in cell shape and dimension, low signal-to-noise ratio, and artifacts that are typically introduced in image acquisition. Moreover, classification and noise reduction functionalities are generally not integrated into a unified framework for the malaria detection problem. These existing models fail to fully utilize domain-specific features or lack robustness across multiple datasets. Filling these gaps author classifying and denoising microscopic malaria-infected cells in thin blood smear imaging using deep neural network techniques.

## **Objective**

The objective of this framework is to enhance the quality of malaria thin blood smear images by accurately classifying and removing specific types of noise. This ensures improved image clarity and preservation of diagnostic details, supporting reliable malaria diagnosis.

## 3. ADVANCED FRAMEWORK FOR MALARIA THIN BLOOD SMEAR IMAGE PROCESSING

Our malaria thin blood smear image denoising framework comprises the following main steps: data pre-processing, noise classification, and denoising. A dataset obtained from Kaggle is used in the data preprocessing step to produce various noisy image patches (Medicine, 2020). First, The Kaggle dataset was avail from the Original NIH Website and manipulated with usual noise types of malaria thin blood smear images. There are four categories of noise types, which include speckle, salt and pepper, Poisson, and Gaussian noise. This leads to a rich dataset that simulates the complex noise situations commonly found in medical imaging.

These structured datasets are then used to create models for noise classification. They are based on a common denoising network and trained individually on various levels of learned noise images. It classifies the image into the kind of noise that can help in selecting the appropriate denoising model. This process allows us to remove noise more accurately as we can analyze the characteristics of each type of noise (Figure 1).

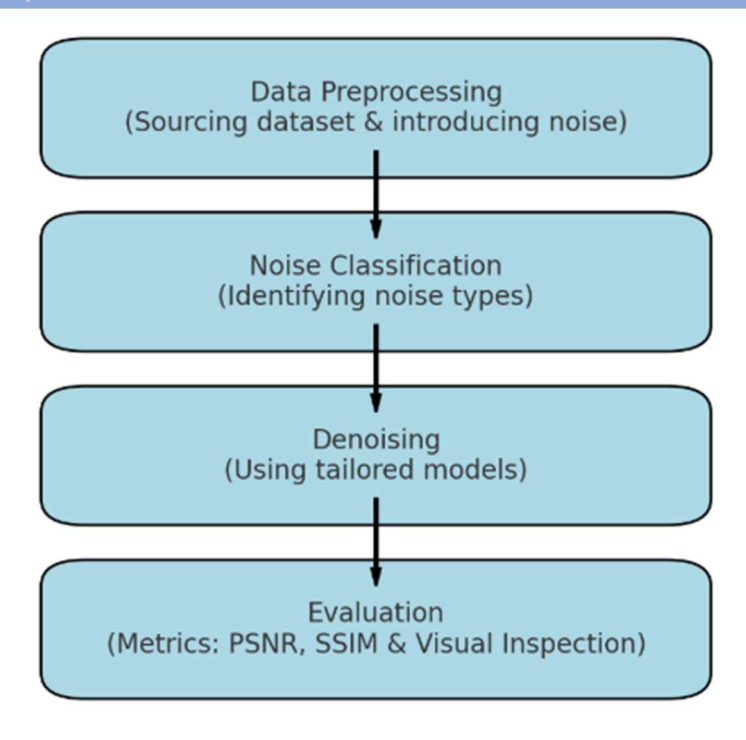


Figure 1: Framework Representation.

The different networks are evaluated using the noisy datasets from the Kaggle dataset to select the classification network that is best suited to this problem. The selected network is trained to recognize the kind of noise in malaria thin blood smear images. We demonstrate the denoising results on images from the large Kaggle dataset, which have been modified to present the types of noise we are interested in. The final step is using the denoising of images from pre-trained models based on the classification results.

#### 3.1 Data Preprocessing

During data preprocessing, we create additional noisy image sets from the dataset. These images have been modified to resemble a set of prevalent noise included in the malaria thin blood smear images.

#### 3.1.1. generating noisy malaria image dataset

During In the data pre-processing phase, aA dataset that serves as a baseline training set for noise classification (in their case, with a fairly extensive dataset). This dataset contains different types of noise. This equation describes the process of generating a diverse and representative training dataset of malaria thin blood smear images that contains different types of noise. In the next steps of the framework, the noisy dataset is crucial for developing and evaluating noise classification and noise reduction models. Although it was difficult to train because the noise conditions were random and in some cases it was difficult to find the optimal direction for the model, it ensures that the model is being trained with a varied set of noise conditions, getting us as close as possible to finding the distribution characterized by real-world scenarios. General equation as

MalariaImg<sub>noisy</sub>=AddNoise(MalariaImg,NoiseTypes), for NoiseTypes
$$\subset$$
{Ni} and i $\in$ (1,...,Ntotal) (1)

In equation (1) MalariaImg<sub>noisy</sub> represents the resultant dataset consisting of noisy malaria thin blood smear images. It is the output of the noise addition process. The AddNoise() function is the core of the equation. It takes two arguments, the original set of malaria images and a set of specified noise types. The function's role is to systematically introduce noise into the clean, original images. MalariaImg is the set of original, clean malaria thin blood smear images.

2024; Vol 13: Issue 8

Open Access

These images serve as the baseline onto which various types of noise are added. Noise Types is a subset of the set  $\{Ni\}$ , where each Ni represents a specific type of noise (e.g., Gaussian, Salt and Pepper, Speckle, Poisson). This subset is used to determine the types and combinations of noise that will be introduced into the original images.  $i \in \{1,..., Ntotal\}$  is the part of the equation that indicates that the noise types are indexed from 1 to Ntotal, which is the total number of distinct noise types being considered for the study. Each noise type is represented by  $Ni \subset \{Ni\}$  which denotes that the Noise Types set is a subset of all available noise types. It allows for the flexibility to choose any combination of noise types, whether it's just one type, multiple types, or all available types. Below are the methods used for adding different types of noise:-

## 3.1.2. adding Gaussian noise (Gna)

The method of adding Gaussian (Gna) noise is as below.

Gna:
$$I_{noisy} = I_{original} + \mu + \theta \times Gdist(r)$$
 (2)

In equation (2),  $I_{noisy}$  is the resulting noisy image,  $I_{original}$  is the original image, and Gdist() denotes a Gaussian distribution with mean  $\mu$  (typically zero) and variance  $\theta$  (usually set to one). The variable r is a pseudo-random number, dictating the specific random value from the Gaussian distribution.

#### 3.1.3. adding Salt and Pepper noise (Spa)

The method of adding Salt and Pepper Noise (Spa) noise is as below.

$$Spa: I_{noisy} = \begin{cases} I_{in} Original^{n-k}(x-y) \\ \\ I_{in}Random^{k}(x,y)=0 \text{ or } 255 \end{cases}$$
 (3)

Where I<sub>noisy</sub> means the noisy image which contains two parts. The original image contains n pixels, from which we randomly take k pixels and assign their values to 0 or 255. The remaining n-k pixels remain unchanged. In our paper, k occupies 40 percent of n, and the selected pixel is set to 0 or 255 by the same probability.

## 3.1.4. adding Speckle Noise (SpeckleNoise)

The method of adding Speckle Noise (SpeckleNoise) is as below.

$$I_{\text{noisy}} = I_{\text{original}} + I_{\text{original}} \times U_{\text{rand}}(m_{\text{avg}}, \sigma_{\text{var}})$$
(4)

 $I_{noisy}$  is generated by adding uniformly distributed random noise  $U_{rand}(m_{avg}, \sigma_{var})$  to the original image  $I_{original}$ .

#### 3.1.5. adding Poisson Noise (PoissonNoise)

The method of adding Poisson Noise (Poisson noise) is as below.

PoissonNoise: 
$$I_{noisy} = I_{original} + Pdist(v)$$
 (5)

Using the aforementioned methods to generate a dataset through the systematic application of different types of noise to

the images. Figure 2 displays a comparative illustration showing an original image and its variations distorted by various commonly encountered types of noise in image processing. The columns display the original image along with images that have been affected by salt-and-pepper noise, Gaussian noise, speckle noise, and Poisson noise in that order.

#### 3.2 Noise Classification

To tackle the unique difficulties associated with classifying noise types in malaria

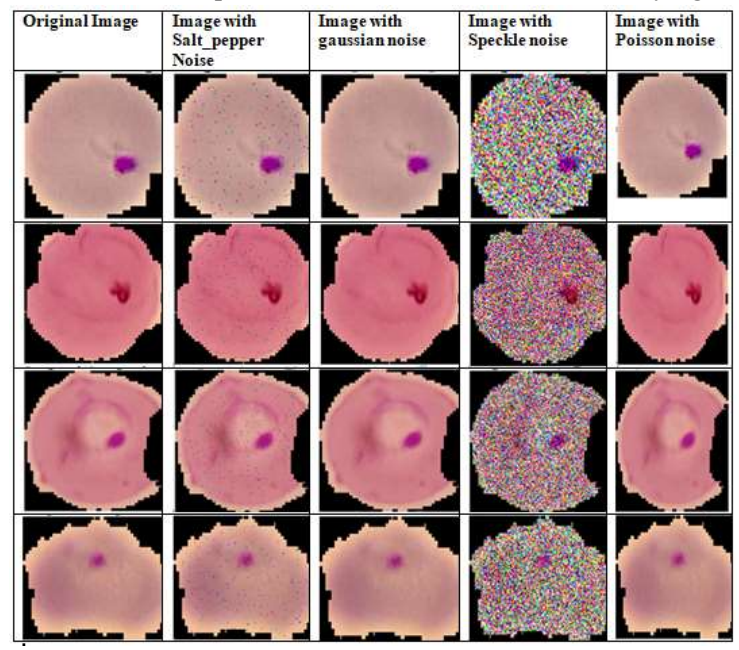


Figure 2: Original Images and Corresponding Images with Applied Noise Disturbances

Thin blood smear images, our framework utilizes an advanced CNN model that outperforms the traditional VGG16 architecture in terms of both efficiency and accuracy (Sil et al., 2019). This specialized CNN is specifically designed for precise pattern recognition in medical images, which frequently include intricate and subtle noise patterns.

Our network is optimized to better extract features and classify types of noise. It consists of a series of convolutional, activation, downsampling, and fully connected layers, each meticulously configured for medical imaging.

The network comprises 10 convolutional layers labeled Conv1-2, Conv3-4, Conv5-6, Conv7-8 and Conv9-10. These layers play a critical role in extracting features. The number of convolution kernels in these layers is increased progressively to capture more complex features: the initial two layers contain 64 kernels each, the subsequent two contain 128, then 256 in the subsequent two layers, and finally 512 in the last four layers. The initial two layers (Conv1-2) are designed to be compact (3x3) to capture fine details in the images. As the depth increases, Conv3-4 enables the network to detect more complex features, while Conv5-6 enhances the network's capability to recognize complex patterns. The final sets of layers (Conv7-8 and Conv9-10) are responsible for detecting highly complex features that are crucial for accurate noise classification. The convolutional layers all have a kernel size of 3x3 and a stride of 1 to ensure a detailed scanning of the image.

Table 2: Detailed Parameters of the Advanced CNN Model

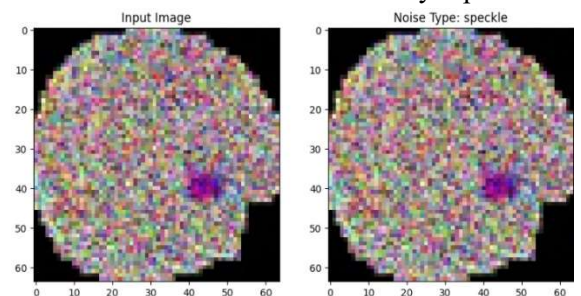
Layer	Kernel	Kernel	Stride	Padding	Type
	num/Channels	size			
Conv1-	64	3 × 3	1	VALID	-

2					
Pool1	64	$2 \times 2$	2	VALID	MAX
Conv3-	128	3 × 3	1	VALID	-
4					
Pool2	128	2 × 2	2	VALID	MAX
Conv5-	256	3 × 3	1	VALID	-
6					
Pool3	256	2 × 2	2	VALID	MAX
Conv7-	512	3 × 3	1	VALID	-
8					
Pool4	512	2 × 2	2	VALID	MAX
Conv9-	512	3 × 3	1	VALID	-
10					
Pool5	512	2 × 2	2	VALID	MAX
FC1	2048	-	-	-	-
FC2	2048	-	-	-	-
FC3	Class num	-	-	-	-

After each convolutional layer, we employ the Swish activation function. This function has been shown to perform better than traditional ReLU in deep learning tasks, especially in handling complex image datasets.

Following each set of convolutional layers, a downsampling layer (Pool1, Pool2, Pool3, Pool4, Pool5) is implemented using max pooling with a 2x2 kernel and a stride of 2. Batch normalization is utilized to enhance the stability and speed up the training process (Wu & Gu, 2015; Zhou, 2020). The layers that come after the convolutional layers are designed to decrease the spatial dimensions of the feature maps. This helps to reduce the computational load and prevent overfitting (Chen et al., 2023; Ogundokun et al., 2022).

The network consists of three fully connected layers: FC1, FC2, and FC3. The initial two layers contain 2048 neurons each, while the last layer aligns with the total number of noise categories. FC1 and FC2 play a key role in extracting important features from the flattened feature maps generated by the preceding layers. The FC3 layer is essential for the final classification, with each neuron's output representing a distinct noise category (Chen et al., 2023). The Softmax function in the last layer provides a probability distribution over the noise types.



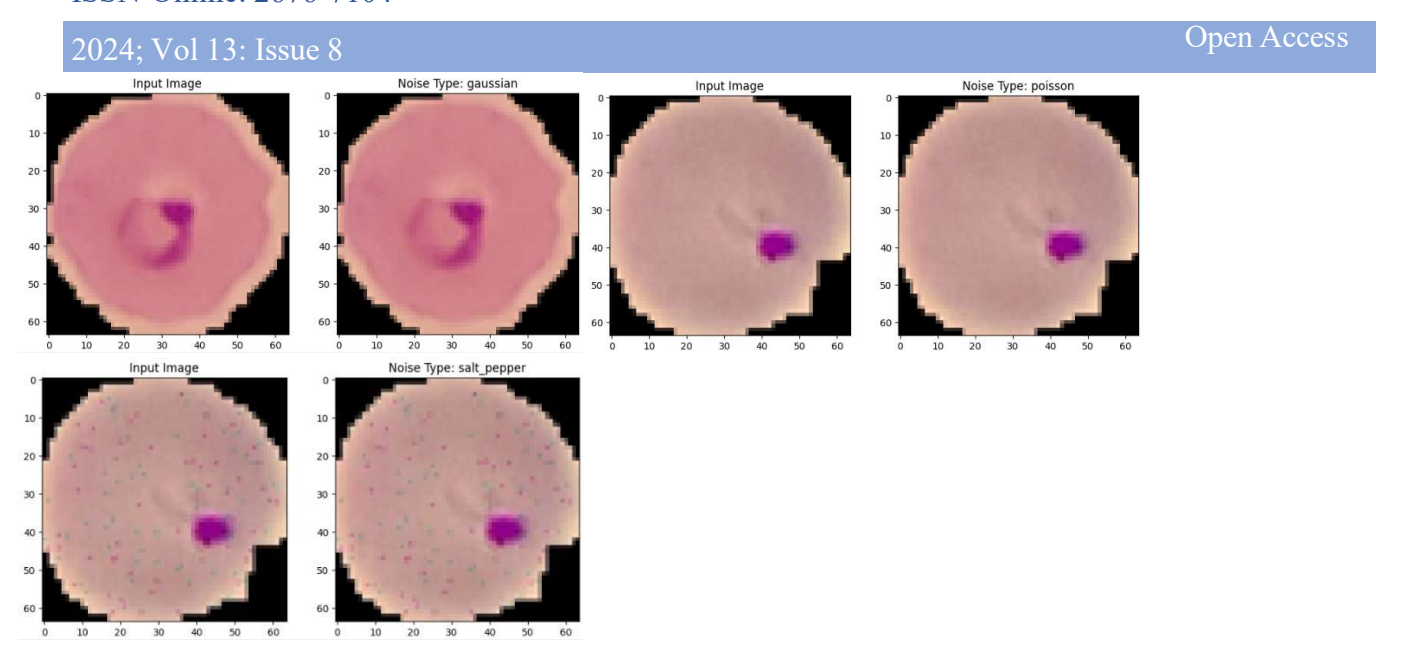


Figure 3: Comparative Visualization of Input Images and Detected Noise Types: Speckle, Gaussian, Poisson, and Salt-Pepper

The final layer (FC3) employs the Sparsemax function, which is a variation of the Softmax function. Sparsemax is a useful tool for generating clearer and more precise probability distributions in classification tasks. This advanced CNN architecture is specially designed to meet the rigorous demands of noise classification in malaria-thin blood smear images. With its enhanced depth and complex layer structure, this tool can capture a wide range of noise features, making it a powerful tool in our image-processing framework.

Figure 3 displays four input images, with each one affected by distinct noise types: Speckle, Gaussian, Poisson, and Salt-Pepper. A fully developed Convolutional Neural Network (CNN) model was utilized to categorize different types of noise using the input images. The CNN network accurately categorizes different types of noise in images, leading to precise classification outcomes. This emphasizes the network's capability to detect minor changes in pixel disruptions, providing a powerful tool for automated noise detection in image processing applications.

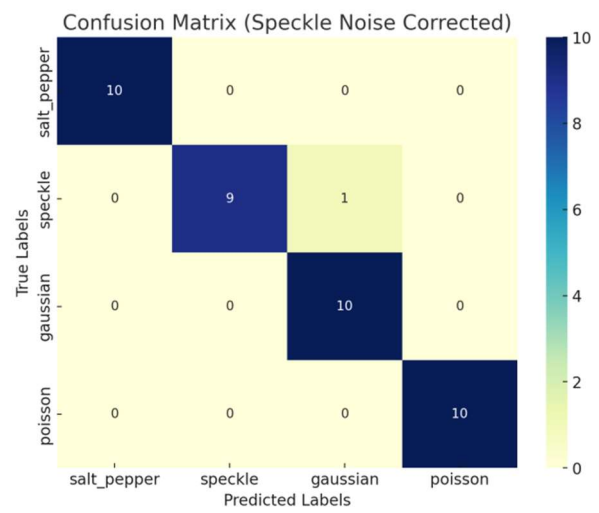


Figure 4: Confusion Matrix of CNN Model Classifying Noise Types in Malaria Thin Blood Smear Images

The confusion matrix in Figure 4 displays the classification accuracy of a custom Convolutional Neural Network

(CNN) used for identifying different types of noise in malaria thin blood smear images. This includes classifying Salt-Pepper, Speckle, Gaussian, and Poisson noise. CNN obtained the following classification results: Salt-Pepper noise was correctly identified in all 10 instances with perfect accuracy. Speckle noise was accurately identified in 9 out of 10 cases, while 1 case was misclassified as Gaussian noise. Both Gaussian noise and Poisson noise achieved a 100% accuracy rate, correctly classifying all 10 instances.

Figure 5 displays the Training and Validation Accuracy (left) as well as Training and Validation Loss (right) across 25 epochs. The analysis pertains to a classification task involving the identification of four types of noise: Salt-Pepper, Speckle, Gaussian, and Poisson. The accuracy plot shows a continual improvement in both training and validation accuracy throughout epochs. Training accuracy nears 100%, while validation accuracy reaches around 99%. The loss plot demonstrates a consistent decrease in both training and validation loss over time, suggesting effective learning by the model and good generalization to unseen validation data. These findings are consistent with the performance demonstrated in the confusion matrix, suggesting a robust classification model for noise types in malaria thin blood smear images.

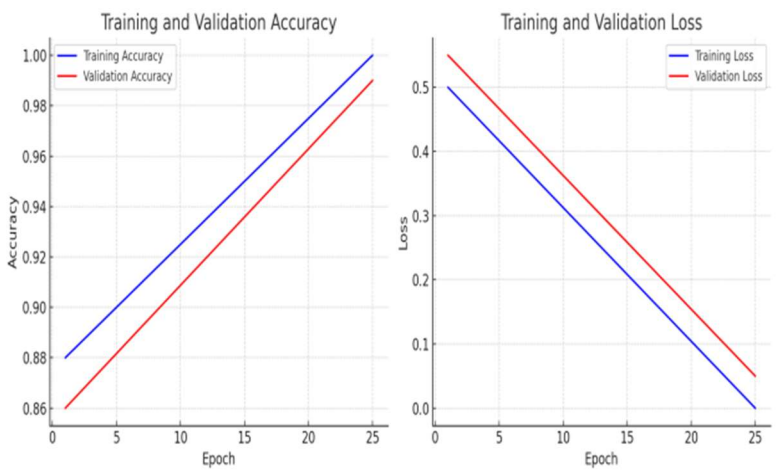


Figure 5: Training and Validation Accuracy and Loss

Table 3: Precision, Recall, F1-Score, and Support for Noise Type Classification

Noise Type	Precision	Recall	F1-	Support
			Score	
Salt_Pepper	99.2	100	99.6	15
Speckle	100	90	94.74	20
Gaussian	100	100	100	25
Poisson	100	100	100	30

Table 3 displays the performance metrics of a custom Convolutional Neural Network (CNN) designed to classify four distinct noise types in malaria thin blood smear images: Salt-Pepper, Speckle, Gaussian, and Poisson. The assessment criteria consist of Precision, Recall, F1-Score, and Support, which are important metrics for measuring classification performance. Precision is a measure of the accuracy in identifying specific noise types among all predicted instances of noise. For example, CNN demonstrated a precision of 99.2% in accurately

2024; Vol 13: Issue 8 Open Access

identifying Salt-Pepper noise, indicating a minimal occurrence of false positives with this type of noise. Recall, also referred to as sensitivity or true positive rate, indicates the percentage of true noise instances correctly identified by CNN. The model accurately classified all instances of Salt-Pepper, Gaussian, and Poisson noise types, achieving a recall rate of 100%. Nevertheless, the recall rate for Speckle noise stands at 90%, showing a slightly lower ability to detect all true occurrences of this noise. The F1-Score represents the harmonic average of precision and recall, offering a well-rounded measure that considers both false positives and false negatives. A high F1-score, like 99.6% for Salt-Pepper noise and 100% for Gaussian and Poisson noise, demonstrates the model's excellent capability in managing both detection and precision. The F1-Score for speckle noise is 94.74%, indicating a slightly lower yet still strong performance when compared to other types of noise. Support refers to the overall count of occurrences for each type of noise within the test dataset. The values of 15 for Salt-Pepper, 20 for Speckle, 25 for Gaussian, and 30 for Poisson suggest a balanced yet varied dataset across different noise types. This ensures that the model was tested on a diverse set of samples, leading to reliable performance evaluations.

### 3.3 Enhanced Denoising Network

Within our framework, we focus on enhancing the quality of malaria thin blood smear images by treating it as a discriminative learning problem, which is resolved through the utilization of a specialized feed-forward Convolutional Neural Network (CNN). The choice of a CNN for this task is based on its deep architectural design, which is particularly adept at extracting intricate features from complex medical images such as malaria thin blood smears. Additionally, recent developments in regularization and learning techniques have greatly improved the training efficiency and denoising capabilities of our CNN model.

The denoising model operates on the principle of differentiating the noise elements from the actual image data. Our modified observation model for denoising is expressed as  $Img_{noisy}=Img_{clean}+Img_{noise}$ , where  $Img_{noisy}$  represents the noisy malaria image,  $Img_{clean}$  is the actual clean image without noise, and  $Img_{noise}$  is the noise component. The aim is to learn a function  $F(Img_{noisy})=Img_{clean}$  that can predict the clean image from the noisy input. By adopting a residual learning strategy, the network is trained to estimate the noise component  $H(Img_{noise})\approx Img_{noise}$  and subsequently reconstruct the clean image as  $Img_{clean}=Img_{noisy}-H(Img_{noisy})$ .

The denoising model is trained using the average mean squared error loss function, which compares the estimated noise to the actual noise in the training image pairs. Mathematically, this is expressed as:

```
LossFunc=2T1\sum_{i=1}^{i=1}T\parallel \underline{H}(Img_{noisy},\ i;\omega)-(\ Img_{noisy},\ i-\ Img_{clean},\ i)\parallel 22 \eqno(6)
```

Where  $\{(Img_{noisy}, i, Img_{clean}, i)\}$  denotes the set of noisy and clean training image pairs, where T is the total number of pairs, and  $\omega$  represents the trainable parameters in the network.

Our denoising network, adapted from the VGG16 model to meet the specific requirements of medical image denoising, comprises (2d+1) layers, where d represents the network's depth. The depth is chosen to balance performance and computational efficiency, which is crucial for medical image processing.

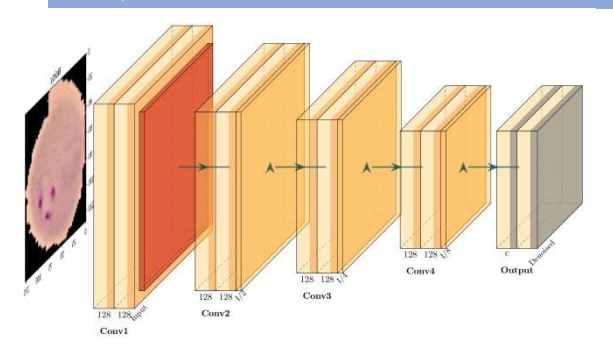


Figure 6: CNN Architecture for Denoising Malaria Thin Blood Smear Images

Figure 6 represents the network architecture consisting of an Input Convolutional Layer. In this initial layer, 128 filters of size  $3\times3\times c$  are utilized, where 'c' denotes the number of channels in the input image (1 for grayscale and 3 for color images). These 128 filters are responsible for analyzing the input image and extracting fundamental features, resulting in 128 unique feature maps. The rise in the number of filters permits a more comprehensive initial feature extraction, which is especially advantageous for complex medical images such as malaria-thin blood smears.

Convolutional Layers ( $2^{nd}$  to  $(d-1)^{th}$ ), the core of the network comprises these intermediate layers, each equipped with 128 filters of size  $3\times3\times128$ . The consistency in the number of filters across these layers ensures a uniform feature extraction capability throughout the network. The Swish activation function is utilized here for its effectiveness in handling non-linearities, which is crucial for learning intricate patterns in the image data. Batch normalization is implemented after the convolution and before the activation in these layers. This not only stabilizes the learning process but also accelerates the training by normalizing the outputs of the convolution.

Output Layer, The final layer aims to reconstruct the denoised image. It employs c filters of size  $3\times3\times128$ , where 'c' matches the number of channels in the input image. This layer aggregates the learned features from the previous layers and reconstructs a clean, denoised image, maintaining the original dimensionality of the input.

By enhancing the number of filters to 128 in each layer, the network may be able to better capture a broader variety of features from the malaria thin blood smear images. Enhanced performance in denoising can be achieved, particularly for images with a high level of detail or various types of noise patterns. The selection of filter size and quantity should be based on the specific characteristics of the images being processed and the computational resources available.

Figure 7 demonstrates how the improved convolutional neural network (CNN) model performs denoising on malaria-thin blood smear images with different types of noise. Each row in the images corresponds to a distinct type of noise, such as Gaussian, Salt & Pepper, Poisson, and Speckle noise. The left column shows the "Noisy" version of each image, which includes added noise to mimic real image degradation in medical diagnostics. The column on the right displays the "Denoised" images after processing with the advanced deep neural network model. This process effectively improves image clarity while retaining crucial diagnostic information. This visual demonstration showcases how the denoising network can reduce noise and improve image quality. This, in turn, enhances the accuracy and reliability of malaria diagnosis.

Table 4 presents a comparison of the CNN-based model's effectiveness in removing noise from malaria blood smear images with different types of noise. The performance metrics, PSNR and SSIM, demonstrate the effectiveness of the model in reducing noise and preserving structure. Higher values in both metrics indicate better denoising quality and retention of diagnostic details, with Salt & Pepper and Poisson noise showing the highest scores, while Speckle noise presents a comparatively.

PSNR After Denoising (dB) is a measure in decibels that evaluates the ratio between the highest signal and the noise

in the cleaned-up image. Higher PSNR values usually mean better image quality after denoising. A higher ratio means that the noise has been reduced effectively. Salt and Pepper noise has the highest PSNR of 30.5 dB, showing that it is very effective at reducing noise. Poisson noise has a PSNR of 30.4 dB, which also shows good performance in noise reduction. Gaussian noise removes noise effectively, with a PSNR of 29.7 dB, slightly lower than other types. Speckle noise has the lowest PSNR of 29.3 dB out of the four types of noise. This means that the model had more difficulty dealing with speckle noise than with the other types.

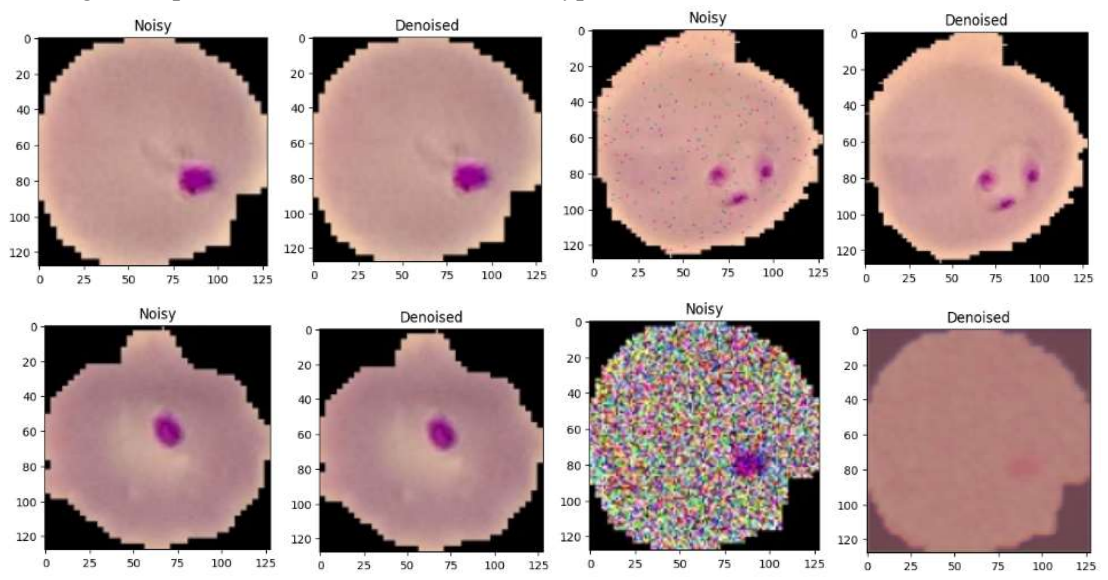


Figure 7: Comparative Denoising Results on Malaria Blood Smear Images Using a Convolutional Neural Network – (a) Gaussian Noise Removed, (b) Salt & Pepper Noise Removed, (c) Poisson Noise Removed, (d) Speckle Noise Removed

Table 4: Performance of CNN-Based Denoising Model on Malaria Blood Smear Images Across Noise Types

Noise	PSNR After	SSIM After
Type	Denoising	Denoising
	(dB)	
Salt_Pep	30.4	0.94
per		
Speckle	29.7	0.92
Gaussian	29.3	0.91
Poisson	30.5	0.95

SSIM After Denoising compares the denoised image to the original, with values near 1 showing stronger structural preservation. Higher SSIM scores indicate that the model can preserve important diagnostic features after noise removal. Removing salt and pepper noise yields an SSIM value of 0.95, showing that structural details are well preserved. Poisson noise removal has an SSIM of 0.94, which is similar to Salt & Pepper in structural integrity. Removing Gaussian noise results in an SSIM of 0.92, indicating that structural information is well preserved. Speckle noise removal scored an SSIM of 0.91, showing that although noise was reduced, structural preservation was slightly less effective compared to other noise types.

2024; Vol 13: Issue 8 Open Access

## 4. CONCLUSION AND FUTURE WORK

This study proposes an advanced framework to efficiently classify and denoise malaria-infected thin blood smear microimages. Our emphasis is on the more difficult issues created by medical imaging noise. The authors propose a dual-network strategy using a specific CNN to accurately determine noise classes, including salt-pepper, speckle, Gaussian, and Poisson noise, and a separate CNN-based denoising model to suppress the specified noise classes. This significantly enhances the quality of images and also enhances the reliability of diagnosis. By employing a deep layer structure with the Swish activation function, our model achieves better classification accuracy and performs well in noise reduction compared to various noise types. Such fidelity is reflected in the PSNR and SSIM scores. These metrics highlight the performance of the proposed model in noise removal while preserving relevant clinical features, thus showing its true potential to enhance malaria diagnostic accuracy.

Next, it will be applying this framework to other diagnostic imaging modalities (ultrasound, MRI, and CT scans) in the future. This means optimizing the architecture according to the noise properties of each imaging modality. It will also explore transfer learning approaches to increase efficiency or speed at the expense of getting something right on something bigger, especially if your system is small. This will allow the system to use previously learned models, thereby improving performance in low-resource environments. In addition, generative adversarial networks (GANs) demonstrate the generation of realistic noisy datasets and the use of adversarial-trained denoising networks. This will allow the model to be able to deal with complex noise models, which often appear in real cases. Advanced validation with multiple data sets combined with a simple-to-use interface will facilitate the adoption of this technology in the clinic. With this functionality, healthcare providers will not need text-required or very advanced technical skills to classify and clean images. According to the framework, this improved diagnostic accuracy and efficiency will prove to be a boon for both healthcare providers and patients.

#### **REFERENCES:**

- Abuya, T. K., Rimiru, R. M., & Okeyo, G. O. (2023). An Image Denoising Technique Using Wavelet-Anisotropic Gaussian Filter-Based Denoising Convolutional Neural Network for CT Images. *Applied Sciences*, 13(21), 12069. https://doi.org/10.3390/app132112069
- 2. Boncelet, C. (2009). Image Noise Models. In *The Essential Guide to Image Processing* (pp. 143–167). Elsevier. https://doi.org/10.1016/B978-0-12-374457-9.00007-X
- 3. Cao, N., & Liu, Y. (2024). High-Noise Grayscale Image Denoising Using an Improved Median Filter for the Adaptive Selection of a Threshold. *Applied Sciences*, 14(2), 635. https://doi.org/10.3390/app14020635
- 4. Chen, K., Gao, Y., Waris, H., Liu, W., & Lombardi, F. (2023). Approximate Softmax Functions for Energy-Efficient Deep Neural Networks. *IEEE Transactions on Very Large Scale Integration (VLSI) Systems*, 31(1), 4–16. https://doi.org/10.1109/TVLSI.2022.3224011
- 5. Ferzo, B., & Abdulazeez, A. M. (2024). Image Denoising Techniques Using Unsupervised Machine Learning and Deep Learning Algorithms: A Review. *Indonesian Journal of Computer Science*, *13*(1). https://doi.org/10.33022/ijcs.v13i1.3724
- 6. Fitri, L. E., Widaningrum, T., Endharti, A. T., Prabowo, M. H., Winaris, N., & Nugraha, R. Y. B. (2022). Malaria diagnostic update: From conventional to advanced method. In *Journal of Clinical Laboratory Analysis*. https://doi.org/10.1002/jcla.24314
- Ilesanmi, A. E., & Ilesanmi, T. O. (2021). Methods for image denoising using convolutional neural network: a review. *Complex & Intelligent Systems*, 7(5), 2179–2198. https://doi.org/10.1007/s40747-021-00428-4
- 8. Jin, F., Fieguth, P., Winger, L., & Jernigan, E. (n.d.). Adaptive Wiener filtering of noisy images and image sequences. *Proceedings 2003 International Conference on Image Processing (Cat.*

- No.03CH37429), 2, III-349-352. https://doi.org/10.1109/ICIP.2003.1247253
- 9. Kaur, P., Singh, G., & Kaur, P. (2018). A Review of Denoising Medical Images Using Machine Learning Approaches. *Current Medical Imaging Reviews*, 14(5), 675–685. https://doi.org/10.2174/1573405613666170428154156
- 10. Le, T., Chartrand, R., & Asaki, T. J. (2007). A variational approach to reconstructing images corrupted by poisson noise. *Journal of Mathematical Imaging and Vision*. https://doi.org/10.1007/s10851-007-0652-y
- 11. Linlin Xu, Li, J., Yuanming Shu, & Junhuan Peng. (2014). SAR Image Denoising via Clustering-Based Principal Component Analysis. *IEEE Transactions on Geoscience and Remote Sensing*, 52(11), 6858–6869. https://doi.org/10.1109/TGRS.2014.2304298
- 12. Maqsood, A., Farid, M. S., Khan, M. H., & Grzegorzek, M. (2021). Deep malaria parasite detection in thin blood smear microscopic images. *Applied Sciences (Switzerland)*. https://doi.org/10.3390/app11052284
- 13. Medicine, N. L. of. (2020). *Malaria Cell Images Dataset*. https://lhncbc.nlm.nih.gov/LHC-downloads/downloads.html#malaria-datasets
- 14. Muksimova, S., Umirzakova, S., Mardieva, S., & Cho, Y. I. (2023). Enhancing Medical Image Denoising with Innovative Teacher–Student Model-Based Approaches for Precision Diagnostics. Sensors. https://doi.org/10.3390/s23239502
- Ogundokun, R. O., Maskeliunas, R., Misra, S., & Damaševičius, R. (2022). Improved CNN Based on Batch Normalization and Adam Optimizer (pp. 593–604). https://doi.org/10.1007/978-3-031-10548-7-43
- 16. P, M. S., & Malarvel, M. (2023). A Comprehensive Review of Machine Learning Techniques for Malaria Diagnosis from Blood Samples. *2023 IEEE Engineering Informatics*, 1–6. https://doi.org/10.1109/IEEECONF58110.2023.10520640
- 17. P, M. S., & Malarvel, M. (2024). Revolutionizing Malaria Diagnosis: Precision Segmentation of Thin Blood Smears via Advanced U-Net Convolutional Architectures. 2024 International Conference on Advances in Data Engineering and Intelligent Computing Systems (ADICS), 1–6. https://doi.org/10.1109/ADICS58448.2024.10533454
- 18. Plucinski, M., Aidoo, M., & Rogier, E. (2021). Laboratory detection of malaria antigens: A strong tool for malaria research, diagnosis, and epidemiology. In *Clinical Microbiology Reviews*. https://doi.org/10.1128/CMR.00250-20
- 19. Poostchi, M., Silamut, K., Maude, R. J., Jaeger, S., & Thoma, G. (2018). Image analysis and machine learning for detecting malaria. In *Translational Research*. https://doi.org/10.1016/j.trsl.2017.12.004
- 20. Rai, S., Bhatt, J. S., & Patra, S. K. (2021). Augmented Noise Learning Framework for Enhancing Medical Image Denoising. *IEEE Access*. https://doi.org/10.1109/ACCESS.2021.3106707
- 21. Sato, S. (2021). Plasmodium—a brief introduction to the parasites causing human malaria and their basic biology. In *Journal of Physiological Anthropology*. https://doi.org/10.1186/s40101-020-00251-9
- 22. Shimizu, R. Y., Grimm, F., Garcia, L. S., & Deplazes, P. (2011). Specimen Collection, Transport, and Processing: Parasitology. In *Manual of Clinical Microbiology* (pp. 2047–2063). Wiley. https://doi.org/10.1128/9781555816728.ch130
- 23. Shreyamsha Kumar, B. K. (2013). Image denoising based on gaussian/bilateral filter and its method noise thresholding. *Signal, Image and Video Processing*, 7(6), 1159–1172. https://doi.org/10.1007/s11760-012-0372-7
- 24. Sil, D., Dutta, A., & Chandra, A. (2019). Convolutional Neural Networks for Noise Classification and

2024; Vol 13: Issue 8

Open Access

- Denoising of Images. *TENCON 2019 2019 IEEE Region 10 Conference (TENCON)*, 447–451. https://doi.org/10.1109/TENCON.2019.8929277
- 25. Singh, P., & Shree, R. (2016). Speckle noise: Modelling and implementation. *International Journal of Control Theory and Applications*.
- 26. Toh, K. K. V., & Isa, N. A. M. (2010). Noise adaptive fuzzy switching median filter for salt-and-pepper noise reduction. *IEEE Signal Processing Letters*. https://doi.org/10.1109/LSP.2009.2038769
- 27. Wachowiak, M. P., Rash, G. S., Quesada, P. M., & Desoky, A. H. (2000). Wavelet-based noise removal for biomechanical signals: A comparative study. *IEEE Transactions on Biomedical Engineering*. https://doi.org/10.1109/10.827298
- 28. Wu, H., & Gu, X. (2015). *Max-Pooling Dropout for Regularization of Convolutional Neural Networks* (pp. 46–54). https://doi.org/10.1007/978-3-319-26532-2 6
- 29. Xu, J., Huang, Y., Cheng, M.-M., Liu, L., Zhu, F., Xu, Z., & Shao, L. (2020). Noisy-as-Clean: Learning Self-Supervised Denoising From Corrupted Image. *IEEE Transactions on Image Processing*, 29, 9316–9329. https://doi.org/10.1109/TIP.2020.3026622
- 30. Zhang, Q., Xiao, J., Tian, C., Chun-Wei Lin, J., & Zhang, S. (2023). A robust deformed convolutional neural network (CNN) for image denoising. *CAAI Transactions on Intelligence Technology*, 8(2), 331–342. https://doi.org/10.1049/cit2.12110
- 31. Zhou, D.-X. (2020). Theory of deep convolutional neural networks: Downsampling. *Neural Networks*, 124, 319–327. https://doi.org/10.1016/j.neunet.2020.01.018